



**HAL**  
open science

## Endonuclease-based genotyping of the RBM as a method to track the emergence or evolution of SARS-CoV-2 variants

Eva Lopez, Margot Barthélémy, Cécile Baronti, Shirley Masse, Alessandra Falchi, Fabien Durbesson, Renaud Vincentelli, Xavier de Lamballerie, Rémi Charrel, Bruno Coutard

### ► To cite this version:

Eva Lopez, Margot Barthélémy, Cécile Baronti, Shirley Masse, Alessandra Falchi, et al.. Endonuclease-based genotyping of the RBM as a method to track the emergence or evolution of SARS-CoV-2 variants. *iScience*, 2021, 24 (11), pp.103329. 10.1016/j.isci.2021.103329 . hal-03524036

**HAL Id: hal-03524036**

**<https://hal.science/hal-03524036>**

Submitted on 5 Jan 2024

**HAL** is a multi-disciplinary open access archive for the deposit and dissemination of scientific research documents, whether they are published or not. The documents may come from teaching and research institutions in France or abroad, or from public or private research centers.

L'archive ouverte pluridisciplinaire **HAL**, est destinée au dépôt et à la diffusion de documents scientifiques de niveau recherche, publiés ou non, émanant des établissements d'enseignement et de recherche français ou étrangers, des laboratoires publics ou privés.



Distributed under a Creative Commons Attribution - NonCommercial 4.0 International License

1           **Endonuclease-based genotyping of the RBM as a method to track the**  
2                           **emergence or evolution of SARS-CoV-2 variants**

3  
4

5 Eva Lopez<sup>1</sup>, Margot Barthélémy<sup>1</sup>, Cécile Baronti<sup>1</sup>, Shirley Masse<sup>2</sup>, Alessandra Falchi<sup>2</sup>, Fabien  
6 Durbesson<sup>3</sup>, Renaud Vincentelli<sup>3</sup>, Xavier de Lamballerie<sup>1</sup>, Rémi Charrel<sup>1,4</sup>, Bruno Coutard<sup>1</sup>

7  
8

9 1 Unité des Virus Émergents (UVE: Aix-Marseille Univ-IRD 190-Inserm 1207), Marseille,  
10 France.

11 2 UR7310, Laboratoire de Virologie, Université de Corse-Inserm, 20250 Corte, France.

12 3 Unité Mixte de Recherche (UMR) 7257, Centre National de la Recherche Scientifique  
13 (CNRS) Aix-Marseille Université, Architecture et Fonction des Macromolécules Biologiques  
14 (AFMB), Marseille, France.

15 4 Comité de Lutte contre les Infections Nosocomiales, Hôpitaux Universitaires de Marseille,  
16 AP-HM, Marseille, France

17

18 **Corresponding author and lead contact:** Bruno Coutard ([bruno.coutard@univ-amu.fr](mailto:bruno.coutard@univ-amu.fr))

19

20 **Abstract**

21 Since the beginning of the Covid-19 pandemics, variants have emerged. Some of them display  
22 increased transmissibility and/or resistance to immune response. Most of the mutations  
23 involved in the functional adaptation are found in the Receptor Binding Module (RBM), close  
24 to the interface with the receptor ACE2. We thus developed a fast molecular assay to detect  
25 mutations in the RBM coding sequence. After amplification, the amplicon is heat-denatured  
26 and hybridized with an amplicon of reference. The presence of a mutation can be detected using  
27 a mismatch-specific endonuclease and the cleavage pattern is analysed by capillary  
28 electrophoresis. The method was validated on RNA of SARS-CoV-2 variants produced *in vitro*  
29 before being implemented for clinical samples. The assay showed 97.8% sensitivity and 97.8%  
30 specificity. The procedure can be set up for high throughput identification of the presence of  
31 mutations and serve as a first-line screening to select the samples for full genome sequencing.

32

33 **Keywords**

34 Variants of Concern, SARS-CoV-2, molecular assay, mutations, Spike protein.

35

36

## 37 **Introduction**

38 In December 2019, individuals with pneumonia of unknown aetiology were recorded in the city  
39 of Wuhan, China. The number of cases increased steadily in the following weeks including in  
40 the countries surrounding China (Taiwan, Thailand, Malaysia, etc.), and then throughout the  
41 world via aerial transport, triggering the WHO to announce a Public Health Emergency of  
42 International Concern (PHEIC) on the 1<sup>st</sup> of February 2020. Shortly after, the disease was  
43 named "COVID-19", for "Coronavirus disease 2019". The coronavirus in question, SARS-  
44 CoV-2, is an enveloped, positive single stranded RNA virus. The viral particle exposes at its  
45 surface the envelope glycoprotein Spike (S). The S protein is a multi-domain protein (Figure  
46 1A) involved in host cell recognition, in particular *via* its receptor binding domain (RBD) which  
47 specifically binds the Human Angiotensin-2 Converting Enzyme (hACE2). The S protein is  
48 considered a major determinant of viral infectivity and antigenicity (Li et al., 2020; Walls et al.,  
49 2020), and mutations in the coding sequence of the S protein are susceptible to affect the biology  
50 of SARS-CoV-2.

51 Since the emergence of SARS-CoV-2 several non-synonymous mutations have been reported  
52 in the coding sequence of the S protein. Some of these non-synonymous mutations are  
53 particularly monitored because they are suspected to affect functions of the protein and thereby  
54 impact the biology of the virus. One of these first mutations led to D614G, a substitution  
55 contributing to the enhancement of viral loads in the upper respiratory tract with possible  
56 increased transmission (Plante et al., 2021). Latter, several variants defined as Variant of  
57 Concern (VoC) have emerged and are disseminating. Those variants may demonstrate increased  
58 transmissibility or severity of the disease, reduction of sero-neutralization by antibodies  
59 induced by previous infection or vaccination, or resistance to therapeutic treatments. Among  
60 the VoCs, the first one - 501Y.V1 or B.1.1.7 lineage - was identified in the UK and showed  
61 enhanced human-to-human transmission and increased disease severity (Davies et al., 2021a)  
62 (Davies et al., 2021b). Then, variants of B.1.351 (501Y.V2), P.1 (501Y.V3) and B.617 lineages  
63 were isolated and characterized in South Africa, Brazil/Japan and India, respectively. Both  
64 B.1.351 (501Y.V2), P.1 (501Y.V3) variants show increased resistance to antibody  
65 neutralization (Davies et al., 2021; Y. Liu et al., 2021; P. Wang et al., 2021). VoCs have in  
66 common to present at least one non-synonymous mutation in the spike receptor binding motif  
67 (RBM). RBM is the sub-domain of the RBD containing most of the hACE2-contacting residues  
68 and is also characterized by the presence of epitopes for neutralising antibodies (Figure 1B).  
69 Some of the characterized mutations are N501Y for 501Y.V1, E484K/N501Y for 501Y.V2 and

70 501Y.V3. By themselves, these mutations can affect the binding of the S protein to hACE2  
71 and/or the potency of neutralizing antibodies (Greaney et al., 2021; Z. Liu et al., 2021; Shang  
72 et al., 2020; P. Wang et al., 2021; Zahradník et al., 2021). The genetic evolution of this region  
73 is specifically scrutinized to identify possible new VoCs. The rapid detection of VoCs is thus  
74 pivotal for mitigating transmission in hospital settings and for adjusting therapies to avoid  
75 lowering efficacy.

76 The detection of VoCs and surveillance of the evolution of SARS-CoV-2 population are  
77 currently surveyed by different approaches. Recently, researchers have developed methods  
78 such as RT-LAMP (LAMP SARS-CoV-2 Variant detection panel, LaCAR), CRISPR-Cas9 or  
79 CRISPR-Cas13-based methods to specifically detect VoCs (Kumar et al., 2021.; Y. Wang et  
80 al., 2021). However the two most commonly used methods are the real time RT-PCR for the  
81 search of mutations at given positions and massive campaigns of New Generation Sequencing  
82 (NGS), both contributing to the public-health decision making (Oude Munnink et al., 2020) .  
83 On one side, real time RT-PCR is fast and operational on site, but it can detect only known  
84 mutations and does not address the newly emerging ones. On the other side, NGS can detect  
85 any mutation along the genome but the results is obtained in days rather than hours, delaying  
86 information required for medical decision to be taken upon sequence identification. In addition,  
87 all the biological samples cannot be sequenced and upstream sampling is mandatory for the  
88 selection of the most relevant biological samples to characterize. Here we present the proof-of-  
89 concept for an alternative method allowing the surveillance of the genetic drift of SARS-CoV-  
90 2 in the RBM region where mutations are susceptible to affect the dissemination, pathogenicity  
91 or antibody-resistance of the virus. The technique, relying on the amplification of the RBM  
92 coding sequence followed by an assay using a mismatch-specific endonuclease, has been  
93 validated on biological samples demonstrating its feasibility.

## 94 **Results and discussion**

### 95 **Principle of the method**

96  
97 Some of the non-synonymous mutations occurring in the RBM coding sequence of SARS-CoV-  
98 2 are pivotal because they are susceptible to change the phenotype with possible influence on  
99 transmission pattern, increased pathogenesis or immune escape; the latter can result in iterative  
100 infections, reduced vaccine efficacy or resistance to Mab-based therapeutics. Accordingly,  
101 RBM genetic evolution has to be monitored for the surveillance of emerging variants. To detect  
102 mutations in the RBM region, we evaluated the SURVEYOR® Nuclease S, an endonuclease

103 cleaving double strand DNA where mismatches exist. The enzyme had already been used for  
104 genotyping for several purposes including the detection of mutations in *brca1* and *brca2* genes  
105 in the case of hereditary breast cancer (Davies et al., 2006; Pilato et al., 2012). The principle of  
106 the technique relies on the creation of heteroduplexes between an amplified DNA from a  
107 reference nucleic acid (*Ref*) and an amplified DNA from a sample to be evaluated (*Sample*).  
108 Both amplicons are mixed (Figure 1C). After denaturation/hybridization, a mixture of  
109 homoduplexes (*Ref/Ref* and *Sample/Sample*) and heteroduplexes (*Ref/Sample*) are produced. If  
110 the sequence from the *Sample* has mutations compared to the *Ref* sequence, mismatches happen  
111 in the heteroduplex. The latter is cleaved, resulting in cleavage products that can be evidenced  
112 by capillary electrophoresis, providing information on the number of Single Nucleotide  
113 Polymorphism (SNPs) and their approximate location(s). In contrast, if the sequences of *Ref*  
114 and *Sample* are identical no cleavage is observed and only the full-length PCR products are  
115 visible by electrophoresis.

116

### 117 **Sensitivity of the RT-PCR assay targeting the RBM coding sequence**

118

119 Within the RBD region of the Spike protein, the RBM contains amino-acids subjected to  
120 mutations (AA) positions – *eg* 452, 484 and 501 - with functional relevance and observed in  
121 VoCs (Figure 1A). Its coding sequence was thus well-suited for a genotyping assay.  
122 Prerequisite was also that the targeted region is centred on the positions of interest and short  
123 enough so that it excludes the identification of mutations with low to no functional effect, *ie*  
124 synonymous or non-synonymous with functional consequence. The size of the PCR product  
125 was thus set to 315-nt, allowing the detection of mutations in the region of the Spike protein  
126 spanning AA positions 431 to 524 of the S protein.

127

128 To set up the assay, we first evaluated the sensitivity of the RT-PCR system in the range 1-10<sup>6</sup>  
129 of RNA copies/μL. The evaluation was done either by real-time RT-PCR with SYBR green  
130 (Figure 2A, 2B), or by end-point analysis of the PCR products on agarose gel electrophoresis  
131 (Figure 2C). The amplification is linear from 10 to 10<sup>5</sup> copies of RNA/μL, with correlation  
132 coefficient R<sup>2</sup>=0.9986 (Figure 2A), and has a limit of detection on agarose gel up to 10  
133 copies/μL (Figure 2C). However, given the quantity of material needed for the nuclease assay  
134 (>25 ng/μL), we arbitrarily applied the threshold at 10<sup>3</sup>/10<sup>4</sup> copies/μL, which corresponds to  
135 samples with Ct values between 28 to 30 in reference detection systems (Pezzi et al., 2020). It  
136 should be noted that the SYBR green inhibits the endonuclease used for the detection of

137 mismatches, likely by altering the structure of the DNA helix, thus rendering the resulting PCR  
138 product not suitable for subsequent capillary electrophoresis analysis (data not shown).

139

## 140 **Detection and identification of mutations revealing in the RBM**

141

### 142 *Detection of mutations in reference material derived from SARS-CoV-2 isolates*

143 To establish the proof of concept, first experiments were conducted using viral RNA derived  
144 from cell cultures infected by three well-characterized variants: SARS-CoV-2 BavPat1,  
145 501Y.V1 and 501Y.V2; (i) 501Y.V1 has N501Y (nt A1501T) mutation, (ii) and 501Y.V2 has  
146 E484K and N501Y (nt G1450A and A1501T, respectively) mutations by reference to the  
147 BavPat1 respectively. The theoretical cleavage profiles for pairwise combinations of the three  
148 variants are presented in Table 1. In practice PCR products were mixed in pairs in approximate  
149 equimolar quantities before denaturation/hybridization prior to the mismatch-specific  
150 endonuclease assay. The results are presented in Figure 2D. The electropherogram (blue curve)  
151 corresponding to the hybridization of the BavPat1 amplicon with itself, with no mismatch  
152 expected, resulted in a unique 330-nt long fragment. When mixed with the one of 501Y.V1 (Fig  
153 2D, orange curve), three DNA fragments were observed at 330, 232 and 93 bp, close to the  
154 anticipated profile (Table 1). For the identification of the 501Y.V2 (grey curve), five DNA  
155 fragments can be detected, corresponding to the products from both complete and partial  
156 cleavages of the mismatches at the expected positions. Finally, when mixing amplicons from  
157 the 501Y.V1 and 501Y.V2 samples (yellow curve), three DNA fragments were observed, where  
158 the two smaller being indicative of the difference at position 484 in the Spike protein sequence  
159 of the two variants.

160

### 161 *Application to clinical samples containing SARS-CoV-2 RNA as diagnosed by routine real-time 162 RT-PCR assay*

163 To further assess the mutation detection method, 8 samples were tested after they were  
164 diagnosed as SARS-CoV-2 RNA positive using the routine diagnostic assay TaqPath real-time  
165 RT-PCR<sup>TM</sup> (ThermoFisher Scientific), known to discriminate the 501Y.V1 variant on the  
166 deletion observed in the S coding sequence, leading to the amplification of only two targets out  
167 the three of the test (Kidd et al., 2021). In order to make the analysis easy and rapid, it is  
168 advocated to test each sample against itself and against the selected reference with no prior  
169 quantification. In our case, the reference was the European lineage of SARS-CoV-2 (BavPat1  
170 strain) since it was the dominant one at the time of the study. Clinical samples were identified

171 as either SARS-CoV-2 positive for the three targets of the TaqPath assay<sup>TM</sup> (Figure 3, samples  
172 1, 3, 4, 5, 7 and 8) or SARS-CoV-2 501Y.V1 positive (Figure 3 samples 2 and 6) with Ct  
173 ranging from 18 to 34. For samples 5 and 8, no fragment corresponding to the expected  
174 amplicon was visible in the self-hybridization assay (Figure 3, lanes 13 and 22), in line with the  
175 high Ct values obtained from initial real time RT-PCR assays. By contrast, the amplification of  
176 the target region for the other sample was satisfactory (Figure 3, lanes 1, 4, 7, 10, 16 and 19).  
177 Overall, SARS-CoV-2 positive and 501Y.V1-putative samples (2 and 6) showed profiles  
178 matching with the expectations, *ie* one mismatch with BavPat1 reference amplicon and no  
179 mismatch with 501Y.V1 reference amplicon (Figure 3, lanes 5, 6 and 17, 18 respectively).  
180 For the other samples (Figure 3, samples 1, 3, 4 and 7), described as non-501Y.V1 according  
181 to the TaqPath assay, no cleavage was expected when compared to the BavPat1 reference  
182 amplicon, and two cleaved products with the 501Y.V1. However, at least one additional  
183 fragment was observed against both reference samples, of about 135 bp length (Figure 3, lanes  
184 2,3,8,9,11,12,20 and 21). The PCR products were submitted to Sanger sequencing and a non-  
185 synonymous mutation yielding S477N substitution was detected, in agreement with the size of  
186 the cleaved products. This mutation had already been reported in viral populations circulating  
187 in Europe (<https://www.gisaid.org/>), and the corresponding variant has been shown to slightly  
188 increase the receptor binding domain's affinity for hACE2 (Hodcroft et al., 2020).  
189 We next blindly evaluated the assay on 92 SARS-CoV-2 positive samples, for which Ct values  
190 were below 28 and NGS data available (Supplemental Figure S1). The sensitivity, defined as  
191 the ability to generate an amplicon with yields compatible for the nuclease assay, is 97.83% as  
192 2 samples out of 92 were not properly amplified. The specificity was defined as the ability to  
193 detect in the RT-PCR-positive samples a mutation compared to the BavPat1 strain or detect the  
194 lack of mutation for sequences identical to the reference. Compared to the sequence data, 2  
195 samples out of 90 were inadequately identified, with selectivity of 97.78%. Out of the 88  
196 remaining profiles, 82 had the same profile as in Figure 2D. Yet unmet patterns were observed  
197 and confirmed by the sequence analysis with E471D mutation detected in two samples, E484K  
198 in one sample, L452R in one sample and both L452R / N501Y in 2 others.  
199 Altogether, these results demonstrate that the mismatch-specific nuclease assay coupled to  
200 capillary electrophoresis is a suitable assay for the detection in clinical samples of already  
201 reported mutations. The identification of atypical profiles, confirmed in this study by  
202 sequencing, also demonstrates that it is relevant for the discovery of yet unmet variants. With  
203 the incremental characterization of variants, the set of reference cleavage patterns can be  
204 updated to adapt the assay to circulating strains. As this technique can be dimensioned for



205 96/384 well devices and requires less than 4 hours from the extracted RNA to production of  
206 individual results, it can be used to filter SARS-CoV-2 positive clinical samples and identify  
207 those for which virus isolation and complete genome sequencing is justified for surveillance  
208 purpose.

209 In conclusion, we developed a molecular assay dedicated to the surveillance of SARS-CoV-2  
210 variants, specifically targeting the RBM coding sequence known to be involved in the  
211 functional adaptation of the virus. The assay is suitable to screen biological samples and identify  
212 the presence new or emerging mutations.

213

### 214 **Limitations of study**

215

216 The technique we developed is based on RT-PCR amplification of the RBM coding sequence  
217 followed by mismatch-specific nuclease assay and detection by DNA capillary electrophoresis  
218 and is made possible only for samples with RNA titers yielding Ct values better than 28 to  
219 produce enough amplified DNA material. The proof of concept has been validated but the  
220 method remains to be deployed on a large cohort to assess if it is amenable to high throughput  
221 genotyping or to individual surveillance of virus evolution during a chronic infection by SARS-  
222 CoV-2, a situation favourable for virus adaptation (Kemp et al., 2021).

223

### 224 **Author contribution**

225

226 B.C conceived the idea and supervised the work. E.L, M.B, C.B, F.D and R.V carried out the  
227 experiments. S.M and A.L provided material on related information. E.L, R.C and B.C wrote  
228 the article. All the authors discussed the results and commented on the manuscript.

229

### 230 **Acknowledgements**

231

232 We thank Professor Bruno Lina and the Centre National de Référence des virus des infections  
233 respiratoires for sharing extracted RNA of clinical samples and sequencing information. This  
234 study was funded by (i) the “European Virus Archive Global” (EVA-GLOBAL) project H2020-  
235 INFRAIA-2019 program, Project No 871029, (ii) the “Advanced Nanosensing platforms for  
236 Point of care global diagnostics and surveillance” (CONVAT), H2020, Project No 101003544.  
237 Eva Lopez is the recipient a DGA fellowship (Direction Générale de l’Armement).

238

## 239 **Declaration of interests**

240 The authors declare no competing interests

## 241 **Figure titles and legend**

242 **Figure 1: RBM is a key region for viral for viral entry and seroneutralization.** A: Primary  
243 structure of the SARS-CoV-2 Spike. NTD: N-terminal domain; RBD: Receptor binding  
244 domain; RBM: Receptor binding motif; SD1: Subdomain 1; SD2: Subdomain 2; FP: Fusion  
245 peptide; HR1: Heptad repeat 1; HR2: Heptad repeat 2; TM: Transmembrane region; CT:  
246 Cytoplasmic region. Amino acid positions of the RBD and RBM boundaries are presented in  
247 black and blue numbers, respectively. Functional mutations in the RBM are shown in orange  
248 (E484K) and red (N501Y). Purple arrows and numbers correspond to the RT-PCR amplified  
249 region. B: Structure representation of the interaction between SARS-CoV-2 RBD core (green)  
250 and hACE2 receptor (white) (PDB 6vw1). RBM is shown in blue. E484 and N501 positions are  
251 highlighted in orange and red, respectively. C: Detection of mutation(s) in a sample compared  
252 to a reference sequence. Results of the digestion by a mismatch-specific endonuclease of an  
253 auto-control (amplicon of a sample alone) and mix (amplicons of reference and sample) are  
254 analysed by electrophoresis and fragment patterns are detected.

255

256 **Figure 2: Evaluation of the target amplification and mismatch-specific nuclease assay on**  
257 **reference material.** A and B: Linearity of the real time RT-PCR assay targeting the RBM  
258 coding sequence from  $10^5$  (blue curve),  $10^4$  (red curve),  $10^3$  (green curve),  $10^2$  (yellow curve)  
259 and  $10^1$  (pink curve) RNA copy/ $\mu$ L. The linear regression (dashed line) in Panel A has a  
260 correlation coefficient  $R^2=0.9986$ . C: End-point analysis of PCR fragments on gel  
261 electrophoresis. D: Electropherograms of the digestion products. Values above the peaks  
262 correspond to the size of the fragment. Peaks on the right (330bp) correspond to the  
263 homoduplexes created during the hybridization.

264 **Figure 3: Validation of the assay on SARS-CoV-2 positive clinical samples.** The First row  
265 indicates number of the samples, from 1 to 8. Ct obtained from TaqPath COVID-19 kit<sup>TM</sup>  
266 (ThermoFisher) real time RT-PCR for ORF1ab, S and N genes are presented in the three next  
267 rows, respectively (nd: not determined, Ct>35), leading to the following classification: (+)  
268 refers to the presence of the deletion indicative of a 501Y.V1 variant, and (-) to a non-501Y.V1

269 sample. Below the table, the results of the mismatch-specific assay followed by capillary  
 270 electrophoresis are presented in a “gel-like” format for the eight samples. The molecular weight  
 271 ladder is indicated on the left. For each sample (1 to 8), the experiment was conducted in three  
 272 conditions: The first lane is the self-hybridization (sample/sample; Lane A), the second one is  
 273 sample/BavPat1 reference (lane B) and the third sample/501Y.V1 reference (Lane C). The  
 274 fragment above 330 bp corresponds to uncleaved homoduplexes.

275

276 **Table 1: Theoretical cleavage profiles for pairwise combinations of amplicons from**  
 277 **BavPat1, 501Y.1 and 501Y.V2 variants.** The amino-acid residue and corresponding position  
 278 in the sequence of the Spike protein for each variant are in italic. Values in the table correspond  
 279 the expected size of the fragments after treatment with the mismatch-specific nuclease.  
 280 Underlined: fragments resulting from the complete cleavage of the heteroduplexes; Bold:  
 281 fragment resulting from an incomplete cleavage.

282

	<i>0</i> <b>BavPat1</b>	<i>N501Y</i> <b>501.V1</b>	<i>E848K ; N501Y</i> <b>501Y.V2</b>
<i>0</i> <b>BavPat1</b>	315	<u>84</u> / <u>231</u> / 315	<u>51</u> / 84 / <b>135</b> / <u>180</u> / <b>231</b> / 315
<i>N501Y</i> <b>501.V1</b>	-	315	<u>135</u> / <u>180</u> / 315
<i>E848K ; N501Y</i> <b>501Y.V2</b>	-	-	315

283

284

## 285 **STAR Methods**

### 286 **Resource availability**

#### 287 *Lead contact*

288 Requests for further information should be directed to Bruno Coutard (bruno.coutard@univ-  
 289 amu.fr).

#### 290 *Materials availability*

291 This study did not generate new unique material or reagents.

## 292 **Data and code availability**

### 293 *Data*

294 All data reported in this paper will be shared by the lead contact upon request.

### 295 *Code*

296 This paper does not report original code.

### 297 *Other items*

298 Any additional information required to reanalyze the data reported in this paper is available  
299 from the lead contact upon request.

## 300 **Experimental model and subject detail**

### 301 *Purified viral RNA from infected cell cultures*

302 VeroE6/TMPRSS2+ (CFAR#100978) cells were grown in minimal essential medium (MEM)  
303 (Thermo Fisher Scientific) with 7.5 % heat-inactivated foetal calf serum (FCS; Thermo Fisher  
304 Scientific), with 1% penicillin/streptomycin (PS, 5000 U.mL<sup>-1</sup> and 5000 µg.mL<sup>-1</sup>  
305 respectively; Thermo Fisher Scientific), supplemented with 1% non-essential amino acids  
306 (Thermo Fisher Scientific) and L-Glutamine (Thermo Fisher Scientific), at 37 °C with 5% CO<sub>2</sub>.  
307 SARS-CoV-2 strain BavPat1 was obtained from Pr. C. Drosten through EVA GLOBAL  
308 (<https://www.european-virus-archive.com/>). SARS-CoV-2 strain 2021/FR/7b-ex UK (EVA-G  
309 ref: 001V-04044) belonging to lineage 501Y.V1 and strain 2021/FR/1299-ex SA (EVA-G ref:  
310 001V-04067) belonging to 501Y.V2 were isolated from Human nasopharyngeal swabs. The  
311 virus stocks were produced on VeroE6/TMPRSS2+ cells. Briefly, a 25 cm<sup>2</sup> flask of sub-  
312 confluent cells was inoculated with each strain at MOI=0.001. Cells were incubated at 37 °C  
313 overnight, after which the medium was changed, and incubation was continued for 24 hours.  
314 The supernatant was then collected, clarified by spinning at 1500 g for 10 min., supplemented  
315 with 25 mM HEPES (Sigma-Aldrich) and stored at -80 °C in several aliquots. All infectious  
316 experiments were conducted in a biosafety level 3 laboratory (BSL3).

### 317 *RNA from clinical samples*

318 For the first set of 8 clinical samples, we collected anonymised residual nasopharyngeal (NP)  
319 samples of COVID-19 patients confirmed by real time RT-PCR from clinical laboratories based  
320 in Corsica in mid-January 2021. No nominative nor sensitive data on participant people have  
321 been collected. This study falls within the scope of the French Reference Methodology MR-  
322 004 according to 2016–41 law dated 26 January 2016 on the modernization of the French health

323 system. The ethics committee of University of Corsica Pascal Paoli (IRB UCPP 2020-01)  
324 approved this study.

325 The collection of 92 SARS-CoV-2 positive clinical samples used in the second evaluation phase  
326 was kindly provided by the National Reference Center for Respiratory Viral Infections (CNR  
327 Lyon, France). The SARS-CoV-2 genomes from the 92 samples were fully sequenced by the  
328 CNR for the surveillance of the variants.

## 329 **Method details**

### 330 *Extraction of the RNA from infected cell cultures*

331 RNA extraction was performed using the QIAamp 96 DNA kit and the Qiacube HT plasticware  
332 kit on the Qiacube HT automate (Qiagen). Viral RNA obtained was quantified by real-time RT-  
333 PCR (EXPRESS One-Step Superscript qRT-PCR Kit (Thermo Fisher Scientific) using 3.5 µL  
334 of RNA and 6.5 µL of qRT-PCR mix and standard fast cycling parameters, i.e., 10 min at 50  
335 °C, 2 min at 95 °C, and 40 amplification cycles (95 °C for 3 sec. followed by 30 sec. at 60 °C)  
336 (Touret et al., 2020). The quantification was provided by four log 2 serial dilutions of an  
337 appropriate T7-generated synthetic RNA standard of known quantities (102 to 108 copies).  
338 Real-time RT-PCR reactions were performed on QuantStudio 12K Flex Real-Time PCR  
339 System (APPLIED BIOSYSTEMS, Waltham, USA) and analysed using QuantStudio 12 K  
340 Flex Applied Biosystems software v1.2.3. Primers and probe targeting SARS-CoV-2 N gene,  
341 are: Forward: 5'-GGCCGCAAATTGCACAAT-3'; Reverse: 5'-CCAATGCGCGACATTCC-  
342 3'; Probe: FAM-CCCCCAGCGCTTCAGCGTTCT-BHQ1.

### 343 *Extraction of the RNA from clinical samples*

344 Total nucleic acids were extracted from 200 µL of NP samples using the QIACUBE processing  
345 system with the QIAamp 96 Virus QIACube HT Kit (Qiagen) and eluted to 100 µL of total  
346 nucleic acid. Real-time RT-PCR was performed for each sample with TaqPath COVID-19  
347 Kit<sup>TM</sup> (Thermo Fisher Scientific). The TaqPath COVID-19 Kit<sup>TM</sup> is a multiplex real time RT-  
348 PCR diagnostic assay targeting three regions of the SARS-CoV-2 genome (N, S, and ORF1ab)  
349 which was approved by the French National Center of respiratory diseases for the detection of  
350 SARS-CoV-2. TaqPath RT-PCR<sup>TM</sup> assay is a useful tool enabling a rapid screening of SARS-  
351 CoV-2 as a S-gene target failure was observed in variants with a deletion at positions 69-70  
352 ( $\Delta$ HV69-70) whereas ORF1ab and N targets are correctly amplified (Bal et al., 2021).

### 353 *Choice of the target sequence for amplification*

354 The target of the SARS-CoV-2 Spike coding sequence ranges from nt position 1273 to 1587,  
355 including the primers, and is 315 nucleotide-long. The corresponding amino acid sequence  
356 (amino acid 425 to 529) encompasses the RBM module (Figure 1A).

357

#### 358 *RT-PCR protocol of the targeted sequence*

359 RT-PCR was performed with SuperScript II One-Step Platinum Kit (#10928042, Thermo  
360 Fisher Scientific), on a Biometra T3000 thermal cycler. Primers were synthesized and provided  
361 by Thermo Fisher Scientific. The forward and reverse primer sequences are: 5'-  
362 TTACCAGATGATTTTACAGGC-3' and 5'-AGACTTTTTAGGTCCACAAAC-3',  
363 respectively. The cycling conditions were defined as follows : 50 °C for 30 min. ; 94 °C for 2  
364 min. ; 40 cycles of 94 °C for 15 sec. ; 55 °C for 20 sec. and 68°C for 20 sec. The final elongation  
365 was performed at 72°C for 2 min.

366

#### 367 *Evaluation of the linearity in the designed system*

368 To determine the linearity of the designed system, real time RT-PCR was performed with  
369 QuantiTect SYBR Green RT-PCR Kit (#204243, Qiagen), on a BioRad CFX96™ thermal  
370 cycler, software version 3.0 (Bio-Rad Laboratories). The cycling conditions were : 50 °C for  
371 30 min. ; 95 °C for 15 min. ; 40 cycles of 95 °C for 15 sec. ; 50 °C for 30 sec. and 72°C for 45  
372 sec. PCR products were then loaded on a 2% agarose gel. The size of the fragment size is  
373 estimated using a molecular size ladder (DNA 1kb Plus #10787026, ThermoFisher Scientific).

#### 374 *Production of the reference PCR products*

375 SARS-CoV-2 BavPat1 strain was selected as the reference for this study. A large scale  
376 production of amplicons was done for this strain, following the RT-PCR protocol defined  
377 above.

#### 378 *Production of the PCR products from biological samples*

379 Each sample used in this study has been amplified following the RT-PCR protocol described  
380 above.

381

382

#### 383 *Mismatch-specific endonuclease assay and detection of cleavage*

384 The presence of a mutation in the amplified target sequence was detected using the Surveyor®  
385 Mutation Detection Kit (#706021, Integrated DNA Technologies). Two PCR products (a  
386 reference product and a sample to be analysed) were mixed in a 10 µL final volume and the

387 endonuclease mismatch specific cleavage was performed following the manufacturer  
388 recommendations. The mixture was then loaded on capillary electrophoresis system (Fragment  
389 Analyser 5200, Agilent or GXII, Perkin Elmer) prior to analysis of the cleavage profile. When  
390 needed for confirmation of the presence of mutations, the PCR products were sequenced using  
391 the Sanger method with the forward and reverse primers used for the RT-PCR (Genewiz).

392

393

## 394 **References**

395 Bal, A., Destras, G., Gaymard, A., Stefic, K., Marlet, J., Eymieux, S., Regue, H., Semanas, Q.,  
396 d'Aubarede, C., Billaud, G., Laurent, F., Gonzalez, C., Mekki, Y., Valette, M.,  
397 Bouscambert, M., Gaudy-Graffin, C., Lina, B., Morfin, F., Josset, L., Group, the C.-  
398 D.H.S., 2021. Two-step strategy for the identification of SARS-CoV-2 variant of  
399 concern 202012/01 and other variants with spike deletion H69–V70, France, August to  
400 December 2020. *Eurosurveillance* 26, 2100008. [https://doi.org/10.2807/1560-](https://doi.org/10.2807/1560-7917.ES.2021.26.3.2100008)  
401 [7917.ES.2021.26.3.2100008](https://doi.org/10.2807/1560-7917.ES.2021.26.3.2100008)

402 Davies, H., Dicks, E., Stephens, P., Cox, C., Teague, J., Greenman, C., Bignell, G., O'Meara,  
403 S., Edkins, S., Parker, A., Stevens, C., Menzies, A., Blow, M., Bottomley, B.,  
404 Dronsfield, M., Futreal, P.A., Stratton, M.R., Wooster, R., 2006. High throughput DNA  
405 sequence variant detection by conformation sensitive capillary electrophoresis and  
406 automated peak comparison. *Genomics* 87, 427–432.  
407 <https://doi.org/10.1016/j.ygeno.2005.11.008>

408 Davies, N.G., Abbott, S., Barnard, R.C., Jarvis, C.I., Kucharski, A.J., Munday, J.D., Pearson,  
409 C.A.B., Russell, T.W., Tully, D.C., Washburne, A.D., Wenseleers, T., Gimma, A.,  
410 Waites, W., Wong, K.L.M., van Zandvoort, K., Silverman, J.D., CMMID COVID-19  
411 Working Group, COVID-19 Genomics UK (COG-UK) Consortium, Diaz-Ordaz, K.,  
412 Keogh, R., Eggo, R.M., Funk, S., Jit, M., Atkins, K.E., Edmunds, W.J., 2021a.  
413 Estimated transmissibility and impact of SARS-CoV-2 lineage B.1.1.7 in England.  
414 *Science*. <https://doi.org/10.1126/science.abg3055>

415 Davies, N.G., Jarvis, C.I., CMMID COVID-19 Working Group, Edmunds, W.J., Jewell, N.P.,  
416 Diaz-Ordaz, K., Keogh, R.H., 2021b. Increased mortality in community-tested cases of  
417 SARS-CoV-2 lineage B.1.1.7. *Nature*. <https://doi.org/10.1038/s41586-021-03426-1>

418 Greaney, A.J., Loes, A.N., Crawford, K.H.D., Starr, T.N., Malone, K.D., Chu, H.Y., Bloom,  
419 J.D., 2021. Comprehensive mapping of mutations in the SARS-CoV-2 receptor-binding  
420 domain that affect recognition by polyclonal human plasma antibodies. *Cell Host*  
421 *Microbe* 29, 463–476.e6. <https://doi.org/10.1016/j.chom.2021.02.003>

422 Hodcroft, E.B., Zuber, M., Nadeau, S., Crawford, K.H.D., Bloom, J.D., Veessler, D., Vaughan,  
423 T.G., Comas, I., Candelas, F.G., Stadler, T., Neher, R.A., 2020. Emergence and spread  
424 of a SARS-CoV-2 variant through Europe in the summer of 2020. *medRxiv*.  
425 <https://doi.org/10.1101/2020.10.25.20219063>

426 Kemp, S.A., Collier, D.A., Datir, R.P., Ferreira, I.A.T.M., Gayed, S., Jahun, A., Hosmillo, M.,  
427 Rees-Spear, C., Mlcochova, P., Lumb, I.U., Roberts, D.J., Chandra, A., Temperton, N.,  
428 CITIID-NIHR BioResource COVID-19 Collaboration, COVID-19 Genomics UK  
429 (COG-UK) Consortium, Sharrocks, K., Blane, E., Modis, Y., Leigh, K.E., Briggs,  
430 J.A.G., van Gils, M.J., Smith, K.G.C., Bradley, J.R., Smith, C., Doffinger, R., Ceron-  
431 Gutierrez, L., Barcenas-Morales, G., Pollock, D.D., Goldstein, R.A., Smielewska, A.,  
432 Skittrall, J.P., Gouliouris, T., Goodfellow, I.G., Gkrania-Klotsas, E., Illingworth, C.J.R.,

433 McCoy, L.E., Gupta, R.K., 2021. SARS-CoV-2 evolution during treatment of chronic  
434 infection. *Nature* 592, 277–282. <https://doi.org/10.1038/s41586-021-03291-y>

435 Kidd, M., Richter, A., Best, A., Cumley, N., Mirza, J., Percival, B., Mayhew, M., Megram, O.,  
436 Ashford, F., White, T., Moles-Garcia, E., Crawford, L., Bosworth, A., Atabani, S.F.,  
437 Plant, T., McNally, A., 2021. S-variant SARS-CoV-2 lineage B.1.1.7 is associated with  
438 significantly higher viral loads in samples tested by ThermoFisher TaqPath RT-qPCR.  
439 *J. Infect. Dis.* <https://doi.org/10.1093/infdis/jiab082>

440 Kumar, M., Gulati, S., Ansari, A.H., Phutela, R., Acharya, S., Azhar, M., Murthy, J., Kathpalia,  
441 P., Kankan, A., Maurya, R., Vasudevan, J.S., S, A., Pandey, R., Maiti, S., Chakraborty,  
442 D., n.d. FnCas9-based CRISPR diagnostic for rapid and accurate detection of major  
443 SARS-CoV-2 variants on a paper strip. *eLife* 10, e67130.  
444 <https://doi.org/10.7554/eLife.67130>

445 Li, Q., Wu, J., Nie, J., Zhang, Li, Hao, H., Liu, S., Zhao, C., Zhang, Q., Liu, H., Nie, L., Qin,  
446 H., Wang, M., Lu, Q., Li, Xiaoyu, Sun, Q., Liu, J., Zhang, Linqi, Li, Xuguang, Huang,  
447 W., Wang, Y., 2020. The Impact of Mutations in SARS-CoV-2 Spike on Viral  
448 Infectivity and Antigenicity. *Cell* 182, 1284-1294.e9.  
449 <https://doi.org/10.1016/j.cell.2020.07.012>

450 Liu, Y., Liu, J., Xia, H., Zhang, X., Fontes-Garfias, C.R., Swanson, K.A., Cai, H., Sarkar, R.,  
451 Chen, W., Cutler, M., Cooper, D., Weaver, S.C., Muik, A., Sahin, U., Jansen, K.U., Xie,  
452 X., Dormitzer, P.R., Shi, P.-Y., 2021. Neutralizing Activity of BNT162b2-Elicited  
453 Serum. *N. Engl. J. Med.* <https://doi.org/10.1056/NEJMc2102017>

454 Liu, Z., VanBlargan, L.A., Bloyet, L.-M., Rothlauf, P.W., Chen, R.E., Stumpf, S., Zhao, H.,  
455 Errico, J.M., Theel, E.S., Liebeskind, M.J., Alford, B., Buchser, W.J., Ellebedy, A.H.,  
456 Fremont, D.H., Diamond, M.S., Whelan, S.P.J., 2021. Identification of SARS-CoV-2  
457 spike mutations that attenuate monoclonal and serum antibody neutralization. *Cell Host*  
458 *Microbe* 29, 477-488.e4. <https://doi.org/10.1016/j.chom.2021.01.014>

459 Oude Munnink, B.B., Nieuwenhuijse, D.F., Stein, M., O’Toole, Á., Haverkate, M., Mollers,  
460 M., Kanga, S.K., Schapendonk, C., Pronk, M., Lexmond, P., van der Linden, A.,  
461 Bestebroer, T., Chestakova, I., Overmars, R.J., van Nieuwkoop, S., Molenkamp, R., van  
462 der Eijk, A.A., GeurtsvanKessel, C., Vennema, H., Meijer, A., Rambaut, A., van Dissel,  
463 J., Sikkema, R.S., Timen, A., Koopmans, M., Dutch-Covid-19 response team, 2020.  
464 Rapid SARS-CoV-2 whole-genome sequencing and analysis for informed public health  
465 decision-making in the Netherlands. *Nat. Med.* 26, 1405–1410.  
466 <https://doi.org/10.1038/s41591-020-0997-y>

467 Pezzi, L., Charrel, R.N., Ninove, L., Nougairede, A., Molle, G., Coutard, B., Durand, G.,  
468 Leparç-Goffart, I., de Lamballerie, X., Thirion, L., 2020. Development and Evaluation  
469 of a duo SARS-CoV-2 RT-qPCR Assay Combining Two Assays Approved by the  
470 World Health Organization Targeting the Envelope and the RNA-Dependant RNA  
471 Polymerase (RdRp) Coding Regions. *Viruses* 12. <https://doi.org/10.3390/v12060686>

472 Pilato, B., De Summa, S., Danza, K., Papadimitriou, S., Zaccagna, P., Paradiso, A., Tommasi,  
473 S., 2012. DHPLC/SURVEYOR Nuclease: A Sensitive, Rapid and Affordable Method  
474 to Analyze BRCA1 and BRCA2 Mutations in Breast Cancer Families. *Mol. Biotechnol.*  
475 52, 8–15. <https://doi.org/10.1007/s12033-011-9468-5>

476 Plante, J.A., Liu, Y., Liu, J., Xia, H., Johnson, B.A., Lokugamage, K.G., Zhang, X., Muruato,  
477 A.E., Zou, J., Fontes-Garfias, C.R., Mirchandani, D., Scharton, D., Bilello, J.P., Ku, Z.,  
478 An, Z., Kalveram, B., Freiberg, A.N., Menachery, V.D., Xie, X., Plante, K.S., Weaver,  
479 S.C., Shi, P.-Y., 2021. Spike mutation D614G alters SARS-CoV-2 fitness. *Nature* 592,  
480 116–121. <https://doi.org/10.1038/s41586-020-2895-3>



481 Shang, J., Ye, G., Shi, K., Wan, Y., Luo, C., Aihara, H., Geng, Q., Auerbach, A., Li, F., 2020.  
482 Structural basis of receptor recognition by SARS-CoV-2. *Nature* 581, 221–224.  
483 <https://doi.org/10.1038/s41586-020-2179-y>

484 Touret, F., Gilles, M., Barral, K., Nougairède, A., van Helden, J., Decroly, E., de Lamballerie,  
485 X., Coutard, B., 2020. In vitro screening of a FDA approved chemical library reveals  
486 potential inhibitors of SARS-CoV-2 replication. *Sci. Rep.* 10, 13093.  
487 <https://doi.org/10.1038/s41598-020-70143-6>

488 Walls, A.C., Park, Y.-J., Tortorici, M.A., Wall, A., McGuire, A.T., Velesler, D., 2020. Structure,  
489 Function, and Antigenicity of the SARS-CoV-2 Spike Glycoprotein. *Cell* 181, 281-  
490 292.e6. <https://doi.org/10.1016/j.cell.2020.02.058>

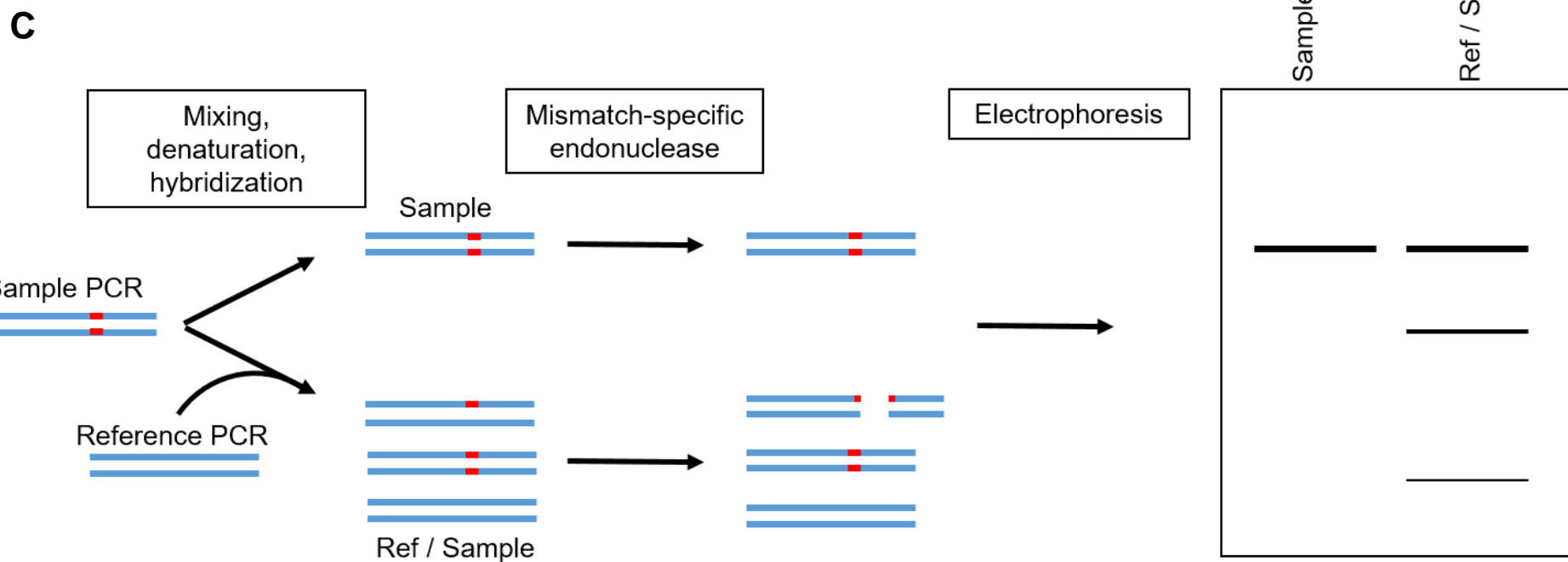
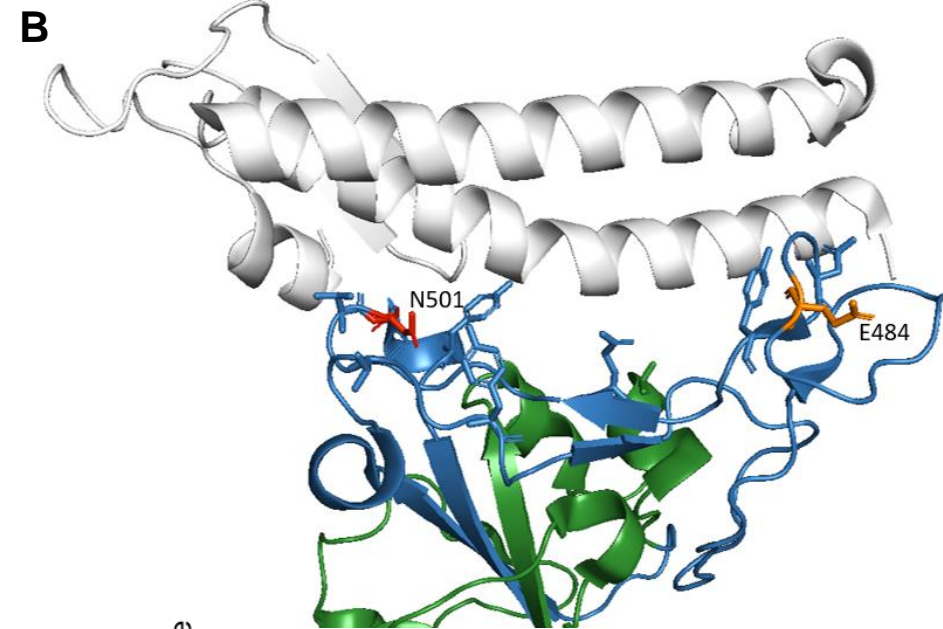
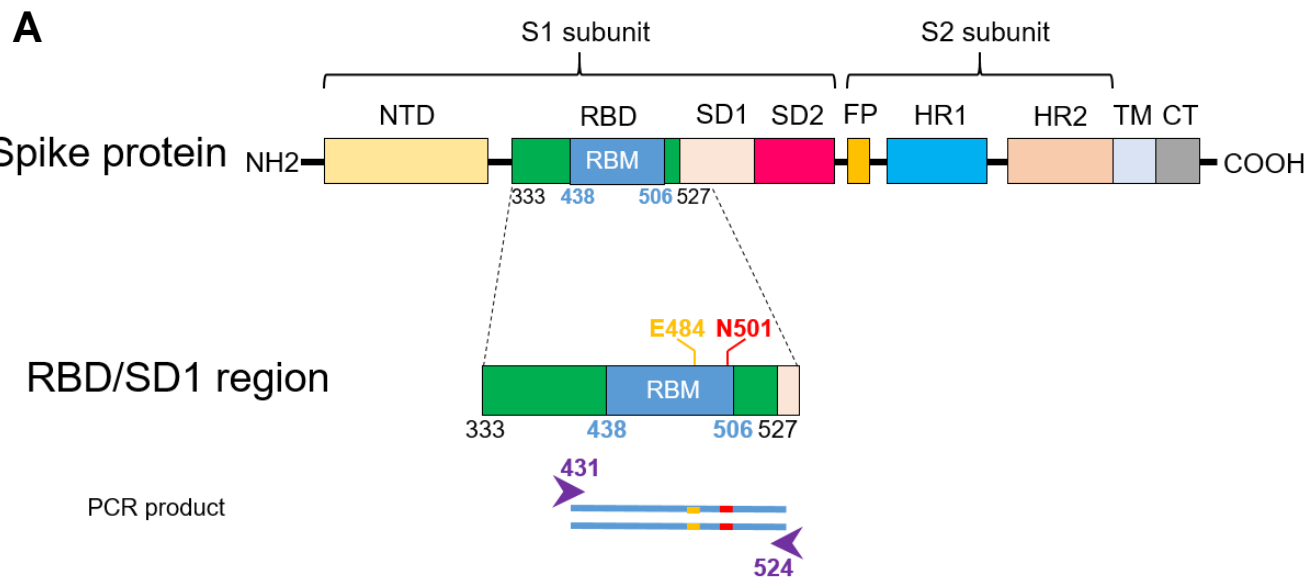
491 Wang, P., Nair, M.S., Liu, L., Iketani, S., Luo, Y., Guo, Y., Wang, M., Yu, J., Zhang, B.,  
492 Kwong, P.D., Graham, B.S., Mascola, J.R., Chang, J.Y., Yin, M.T., Sobieszczyk, M.,  
493 Kyratsous, C.A., Shapiro, L., Sheng, Z., Huang, Y., Ho, D.D., 2021a. Increased  
494 Resistance of SARS-CoV-2 Variants B.1.351 and B.1.1.7 to Antibody Neutralization.  
495 *BioRxiv Prepr. Serv. Biol.* <https://doi.org/10.1101/2021.01.25.428137>

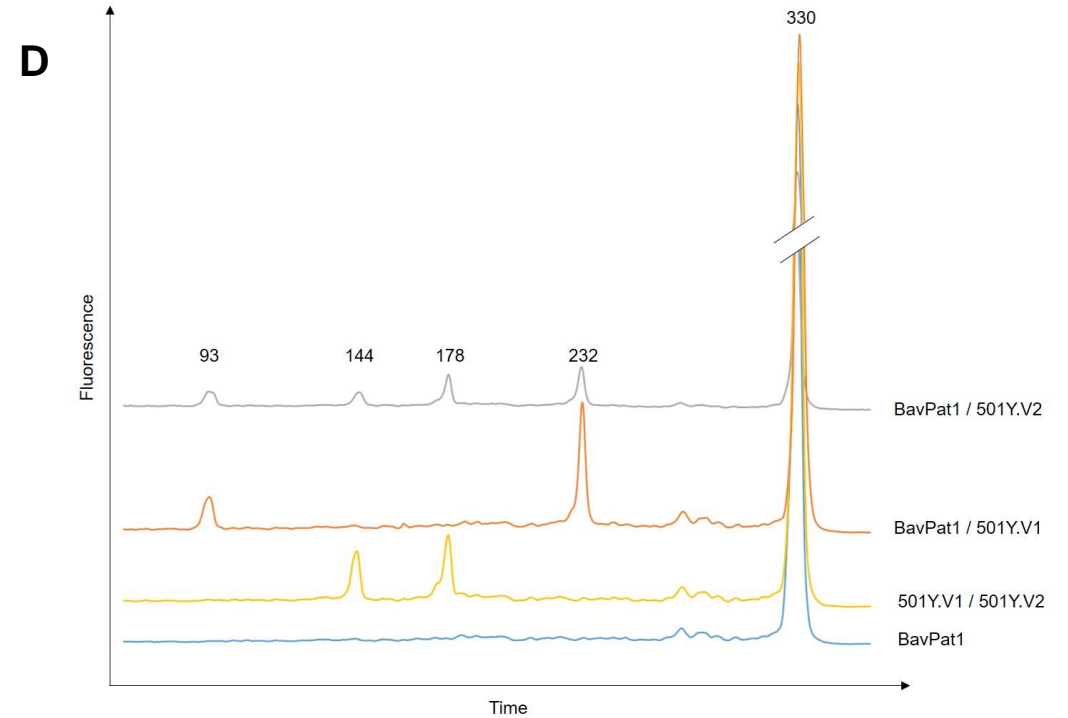
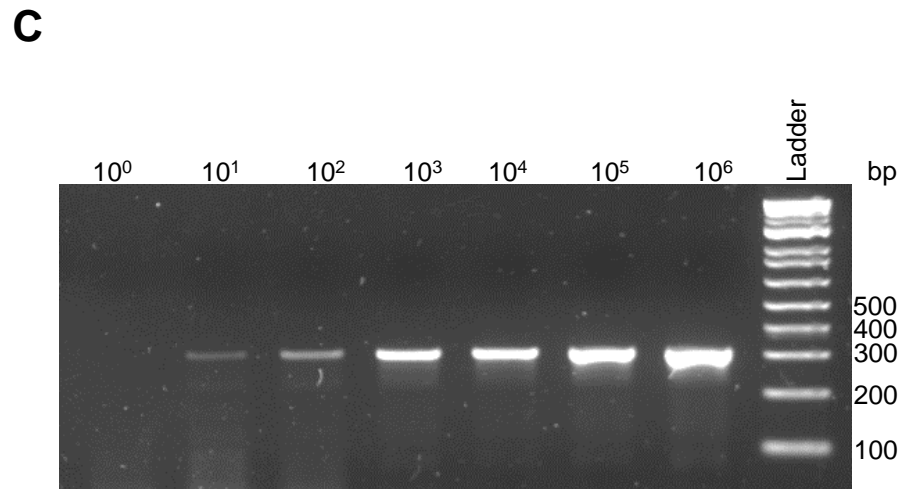
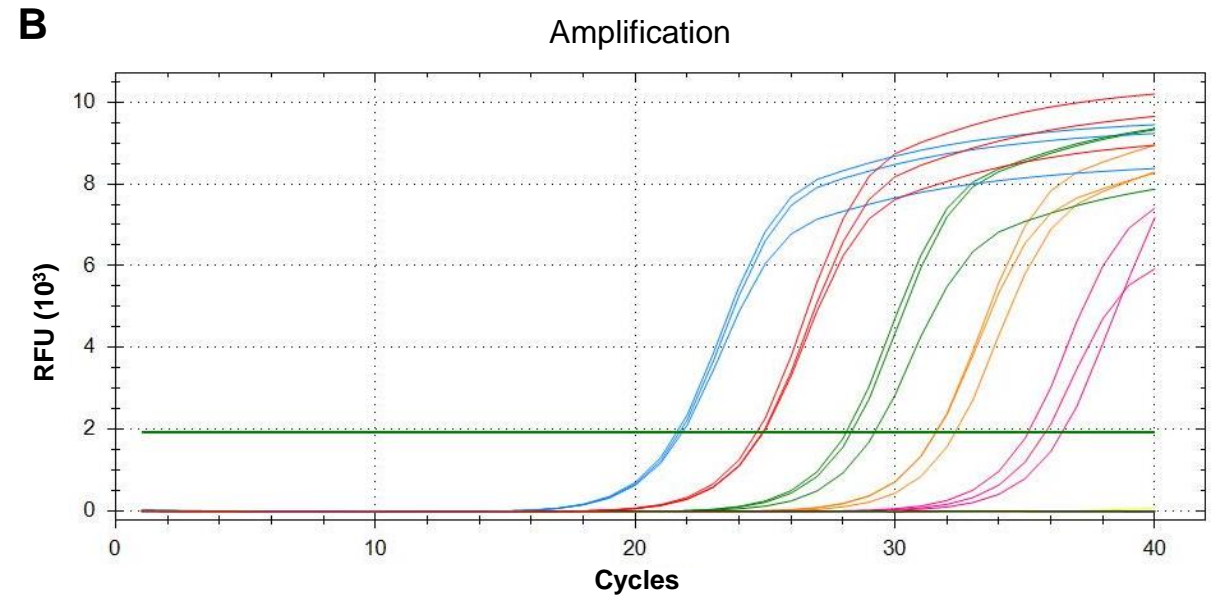
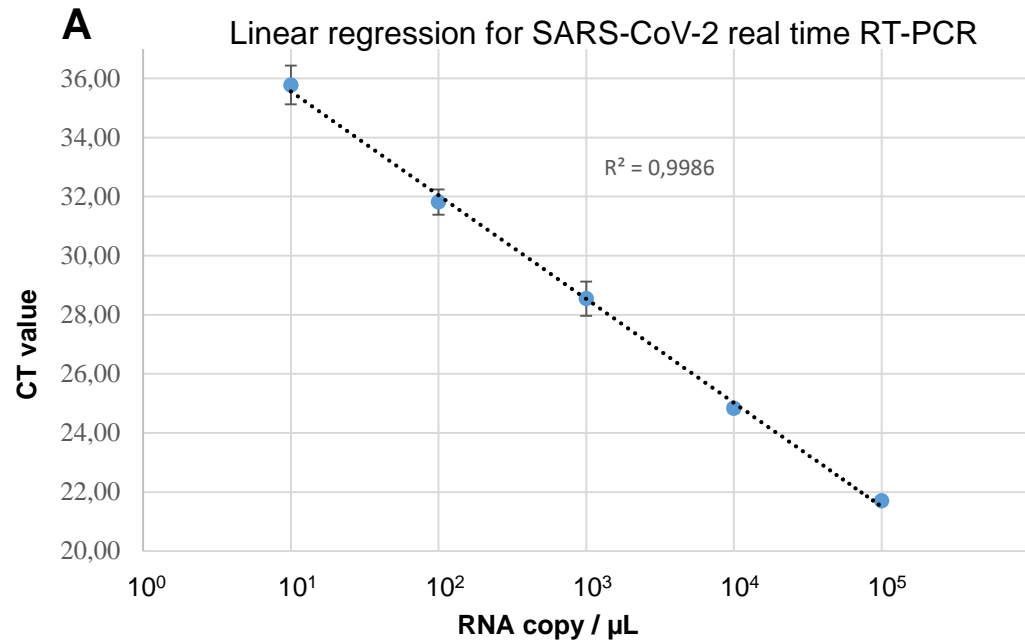
496 Wang, P., Nair, M.S., Liu, L., Iketani, S., Luo, Y., Guo, Y., Wang, M., Yu, J., Zhang, B.,  
497 Kwong, P.D., Graham, B.S., Mascola, J.R., Chang, J.Y., Yin, M.T., Sobieszczyk, M.,  
498 Kyratsous, C.A., Shapiro, L., Sheng, Z., Huang, Y., Ho, D.D., 2021b. Antibody  
499 Resistance of SARS-CoV-2 Variants B.1.351 and B.1.1.7. *bioRxiv* 2021.01.25.428137.  
500 <https://doi.org/10.1101/2021.01.25.428137>

501 Wang, Y., Zhang, Y., Chen, J., Wang, M., Zhang, T., Luo, W., Li, Y., Wu, Y., Zeng, B., Zhang,  
502 K., Deng, R., Li, W., 2021. Detection of SARS-CoV-2 and Its Mutated Variants via  
503 CRISPR-Cas13-Based Transcription Amplification. *Anal. Chem.*  
504 [acs.analchem.0c04303](https://doi.org/10.1021/acs.analchem.0c04303). <https://doi.org/10.1021/acs.analchem.0c04303>

505 Zahradník, J., Marciano, S., Shemesh, M., Zoler, E., Chiaravalli, J., Meyer, B., Rudich, Y.,  
506 Dym, O., Elad, N., Schreiber, G., 2021. SARS-CoV-2 RBD in vitro evolution follows  
507 contagious mutation spread, yet generates an able infection inhibitor. *bioRxiv*  
508 2021.01.06.425392. <https://doi.org/10.1101/2021.01.06.425392>

509





Samples	1	2	3	4	5	6	7	8
<b>TaqPath COVID-19 kit™ , Ct values for each gene</b>								
<b>ORF1ab</b>	24	21	25	22	30	23	27	34
<b>S</b>	24	nd	25	22	30	nd	27	34
<b>N</b>	23	18	24	22	30	22	27	34
<b>Presence (+) or absence (-) of the deletion indicative of 501Y.V1</b>								
<b>501Y.V1</b>	(-)	(+)	(-)	(-)	(-)	(+)	(-)	(-)

